

A generalized perturbation approach for exploring stock recruitment relationships

Justin D. Yeakel · Marc Mangel

Received: 17 September 2013 / Accepted: 20 June 2014
© Springer Science+Business Media Dordrecht 2014

Abstract Models of stock-recruitment relationships (SRRs) are often used to predict fish population dynamics. Commonly used SRRs include the Ricker, Beverton-Holt, and Cushing functional forms, which differ primarily by the degree of density-dependent effects (compensation). The degree of compensation determines whether recruitment respectively decreases, saturates, or increases at high levels of spawning stock biomass. In 1982, J.G. Shepherd united these dynamics into a single model, where the degree of compensation is determined by a single parameter. However, the difficulty in relating this parameter to biological data has limited its usefulness. Here, we use a generalized modeling framework to show that the degree of compensation can be related directly to the functional elasticity of growth, which is a general quantity that measures the change in recruitment relative to a change in biomass. We show that the elasticity of growth can be calculated from perturbations in fish biomass, is robust to observation error,

and can be used to determine general attributes of the SRR in both continuous time production models, as well as discrete time age-structured models.

Keywords Compensatory dynamics · Generalized modeling · Stock-recruitment relationships · Shepherd function · Neimark-Sacker bifurcation

Introduction

Recruitment plays a central role in population dynamics (Gulland 1988). Models of fish recruitment include both density-independent and density-dependent effects. When density-dependent effects are negligible, recruitment is generally modeled as $S(B) = \alpha B$, where $S(B)$ is the level of recruitment when B is spawning stock biomass, and α is the recruitment rate in the absence of density-dependent effects (e.g., Sissenwine and Shepherd 1987). We note that recruitment functions are often introduced as $R(B)$, but to prevent confusion later on (where we introduce scaled functions denoted by lowercase letters, such that r could be confused as a population growth rate), we avoid the use of R to denote recruitment. In using spawning stock biomass, we have followed a relatively standard assumption of fishery science that fecundity is proportional to biomass (as are other measures such as total egg production; Marshall 2009).

When density-dependent effects are non-negligible, recruitment is anticipated to deviate from this relationship, such that $S(B) = \alpha BF(\beta, B)$, where the function F controls density-dependent effects on recruitment and β measures the intensity of density-dependent factors. Traditional stock recruitment models introduce three general kinds of density-dependent responses to increasing spawning stock

J. D. Yeakel (✉)
Center for Stock Assessment Research and Department of Ecology and Evolutionary Biology, University of California Santa Cruz, Santa Cruz, CA 95064, USA
e-mail: jdyeakel@gmail.com

J. D. Yeakel
Santa Fe Institute, Santa Fe, NM 87501, USA

M. Mangel
Center for Stock Assessment Research and Department of Applied Mathematics and Statistics, University of California Santa Cruz, Santa Cruz, CA 95064, USA
e-mail: msmangel@ucsc.edu

M. Mangel
Department of Biology, University of Bergen, Bergen 5020, Norway

biomass: (1) recruitment increases to a maximum and then declines, (2) recruitment saturates, and (3) recruitment continues to increase but at a lower rate than in the absence of density-dependent effects (Shepherd 1982). These alternative scenarios thus differ in the intensity of density dependence (degree of compensation), which determines to what extent recruitment is altered as a function of spawning stock biomass.

Ricker (1954) developed a stock-recruitment relationship (SRR) to introduce declines in recruitment at high levels of spawning stock biomass (Fig. 1a),

$$S(B) = \alpha B e^{-\beta B}. \tag{1}$$

As spawning stock biomass increases, recruitment increases to the maximum $S(B) = 1/\beta$ and then declines. The Ricker model is used if there are predatory response lags, when greater stock abundance suppresses juvenile growth or when cannibalism or nest predation limits recruitment when B is high (Cushing 1988).

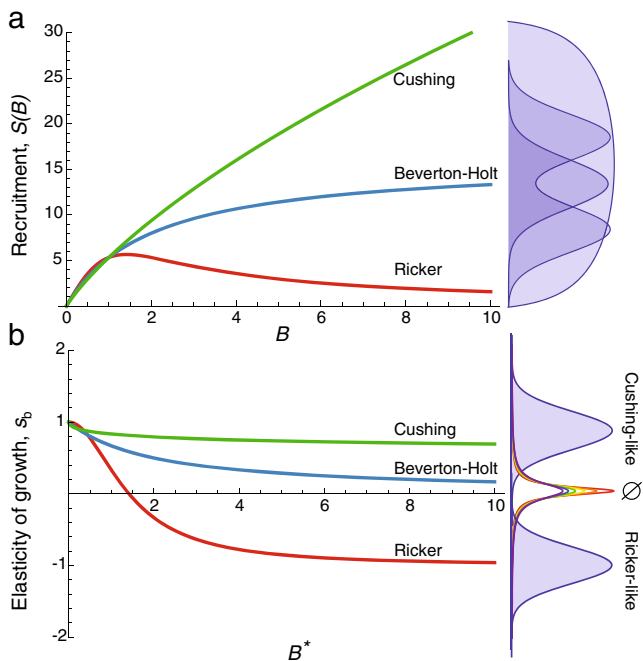


Fig. 1 **a** Recruitment $S(B)$ as a function of spawning stock biomass B . **b** The elasticity of growth s_b as a function of the steady state spawning stock biomass B^* . The distributions to the right represent potential measurements of recruitment **a** and the elasticity of growth **b** for Ricker, B-H, and Cushing recruitment functions. Although measurements for SRRs overlap in **a**, the elasticities of the Ricker- and Cushing-like functional families can be represented by non-overlapping intervals. Ricker: $s_b \in [-\infty, 0)$; Cushing: s_b in $(0, \infty]$; the B-H function is the boundary between Ricker- and Cushing- functional families, such that $s_b \in \emptyset$. The multi-colored distribution emphasizes that the elasticity of growth for the B-H SRR at increasing levels of spawning stock biomass becomes a null set (warmer colors of the distribution), such that the area under the curve becomes infinitesimally small

Beverton and Holt (1957) introduced a related two parameter model where

$$S(B) = \frac{\alpha B}{1 + \beta B}. \tag{2}$$

Recruitment is thus a saturating function of spawning stock biomass, where saturation occurs at $S(B) = \alpha/\beta$ as $B \rightarrow \infty$. In this case, one assumes that density-dependent mortality affects recruitment instantaneously (see Mangel et al. 2006) and that recruitment tends asymptotically towards a finite value as B increases (Cushing 1988). The Beverton-Holt (B-H) relationship is typically used if recruitment is assumed to be limited primarily by food or habitat resources (Shepherd 1982). Note that when βB is small, so that the exponential in Eq. 1 or the denominator in Eq. 2 are Taylor expanded, we obtain $S(B) = \alpha B(1 - \beta B)$, thus giving interpretation to the standard logistic model of population growth.

In open systems where resources are not locally limiting, Cushing (1973) developed a power-law SRR

$$S(B) = \alpha B(\beta B)^{-1/n_c} = \alpha \beta^{-1/n_c} B^{\frac{n_c-1}{n_c}}. \tag{3}$$

Here, the third parameter n_c controls the rate of recruitment increase at high biomass densities or the degree of compensation. In this case, if $n_c > 1$ recruitment continues to increase with increasing spawning biomass, but at a decreasing rate.

In an attempt to integrate the above relationships into a single function controlled by the degree of compensation, Shepherd (1982) observed that the behaviors exhibited by the Ricker, Cushing, and Beverton-Holt functions can be united into a single framework with three free parameters

$$S(B) = \frac{\alpha B}{1 + \beta B^{1/n}}, \text{ for } n > 0. \tag{4}$$

The parameters α and β again denote the initial rate of growth and the effects of density-dependence, respectively, while n is the degree of compensation. When $n < 1$, recruitment increases when B is low, and decreases when B is high, similar to the Ricker function. When $n = 1$, Eq. 4 is the Beverton-Holt (B-H) SRR, where recruitment saturates as B increases. For values of $n > 1$, recruitment behaves similarly to the Cushing function, maintaining a positive slope as B increases. The versatility of the Shepherd function comes at the cost of the additional degree of compensation parameter, which is often difficult to relate to observational data and this has served to limit its adoption.

Using observational data, we are often unable to distinguish which model is most descriptive of the underlying dynamics. This has been a long-standing problem: in 1982, Gulland noted that “in many cases, the variability of the

data makes it difficult to choose between alternative mathematical models” (pg. 17). Such variation may arise from changes in productivity (Dorner et al. 2008), phenotypic variability (Johnson et al. 2014), or differences in life-history (Moore et al. 2014). For instance, SRRs may be constrained by multiple, rather than a single compensatory event (Brooks and Powers 2007), and these species-specific characteristics can be controlled by many different aspects of fish reproductive biology (Morgan et al. 2011). In cases such as these, more complex models may be required, but this is at the cost of additional parameters, limiting the model’s applicability to different systems. Distinguishing between possible compensatory scenarios without assuming knowledge of the exact form of the SRR will thus provide insight into the population dynamics of a fish species. Bayesian nonparametric techniques provide one way to estimate descriptive characteristics of stock-recruitment functions based only on the data (Munch et al. 2005). Such approaches are extremely useful as predictive tools (Perretti et al. 2013a, b), but by definition cannot shed light on the mechanistic processes underlying stock-recruitment dynamics.

Here, we present an analytical approach to determine compensatory dynamics, without assuming knowledge of the specific SRR. We use a generalized modeling framework (*sensu* Gross and Feudel 2006; Gross et al. 2009; Stiefs et al. 2010; Yeakel et al. 2011; Kuehn et al. 2013) to derive relationships between the degree of compensation and the functional elasticities (the logarithmic derivative of a function, giving a measure of the change of the function relative to a change in its argument) of a continuous time generalized production model, as well as a discrete time age-structured model. Our results demonstrate that families of SRRs can be distinguished by these functional elasticities, which can be estimated from the dynamics of perturbations in fish biomass. We also show that some stock-recruitment families can be distinguished more easily than others, and that these differences are closely related to the stability of populations controlled by different compensatory dynamics. Our use of generalized modeling in this context lends clarity to the observation that the Beverton-Holt function is qualitatively different than either the Ricker or Cushing functions, existing as a boundary between two distinct functional families, which leads to different expectations for measuring SRRs in nature.

We emphasize that the approach presented here is an alternative to—and not a replacement of—traditional methods of exploring SRRs in fisheries. In his 1948 introduction to a space-time approach to non-relativistic quantum mechanics, Richard Feynman wrote “*The formulation is mathematically equivalent to the more usual formulations... However, there is a pleasure in recognizing old things from a new point of view. Also, there are problems for which the*

new point of view offers a distinct advantage.” (Feynman 1948, pg 367). It is in this spirit that the use of elasticities to investigate fisheries SRRs provides a “different point of view” to an old problem. Our approach may offer certain advantages, particularly when time-series data are limited, or when historical fluctuations of population trajectories do not obtain very low or very high values, such that traditional methods of fitting SRRs are unsuited. Thus, our present aim is to introduce a new perspective from which to investigate the compensatory dynamics of fish populations.

Methods and analysis

Despite the intrinsic simplifications introduced when using production or biomass dynamic models, they can offer direct insight into the mechanisms governing fish recruitment and thus remain an important and oft-used tool in fisheries management (Mangel et al. 2002, 2013), so we begin with them. We then extend our results and methods to a discrete time age-structured system and show how functional elasticities can distinguish between stock-recruitment families and provide direct insight into the stability regimes of populations with complex life histories.

Analysis of a generalized stock-recruitment model

In a generalized production model, we assume that biomass enlarges according to the function $S(B)$ and shrinks according to the function $D(B)$, such that biomass changes as

$$\frac{d}{dt}B = S(B) - D(B). \quad (5)$$

The enlargement function $S(B)$ may be assumed to have Ricker, B-H, or Cushing recruitment dynamics, whereas $D(B)$ is often assumed to be linear, such that $D(B) = zB$, where z is the rate of biomass loss due to fishing, natural mortality, or a combination thereof. However, in many cases, we cannot assign a specific function to either $S(B)$ or $D(B)$. The analysis of such a general model is not straightforward, since the steady-state solution (B^* , where $S(B^*) = D(B^*)$) cannot be described analytically. In contrast, specific models present essentially the opposite problem: a steady-state solution can often be computed, however the specific mathematical relationships may not accurately represent the dynamics of the population.

The general model presented in Eq. 5 cannot be solved at the steady state because the functions are unknown. However, we can identify the unknown steady state(s) with the variable B^* . If we assume that $B^* > 0$ and that the signs of the growth and loss functions are biologically meaningful, then we can normalize the system to B^* . This allows us to

define a set of normalized variables and functions. We set $S^* = S(B^*)$ and $D^* = D(B^*)$, and define

$$b = \frac{B}{B^*}, \quad s(b) = \frac{S(B)}{S^*}, \quad \text{and} \quad d(b) = \frac{D(B)}{D^*}. \quad (6)$$

This normalization procedure enables consideration of *all positive steady states* in the whole class of systems defined by Eq. 5, with the important property that at the steady state all generalized functions and variables are equal to unity [$b = 1, s(1) = 1, d(1) = 1$]. By substituting the normalized variables into Eq. 5, we obtain the normalized general production model

$$\frac{d}{dt}b = \frac{S^*}{B^*}s(b) - \frac{D^*}{B^*}d(b), \quad (7)$$

and under steady-state conditions ($b = s(b) = d(b) = 1$), this simplifies to

$$0 = \frac{S^*}{B^*} - \frac{D^*}{B^*}. \quad (8)$$

Thus, at the steady state, the scaled growth and mortality coefficients are equivalent, allowing us to define the timescale of the system

$$\gamma = \frac{S^*}{B^*} = \frac{D^*}{B^*}. \quad (9)$$

This parameterization is useful because γ has a biologically relevant interpretation and represents the biomass turnover rate at the steady state. That is, for example, S^*/B^* has units of production per unit of time of new biomass per unit of existing biomass.

In generalized modeling, coefficients such as γ are referred to as “scale parameters” (Gross and Feudel 2006). Substituting γ into Eq. 7, the generalized equation is

$$\frac{d}{dt}b = \gamma(s(b) - d(b)). \quad (10)$$

Although the normalized functions $s(b)$ and $d(b)$ are still unknown, we can assess the dynamics of Eq. 10 by investigating the system under a small perturbation evaluated at the steady state, accomplished by taking the derivative of the normalized system. The derivative of the right hand side of Eq. 10 evaluated at the steady state is

$$\lambda|_* = \gamma \left(\left. \frac{\partial s(b)}{\partial b} \right|_* - \left. \frac{\partial d(b)}{\partial b} \right|_* \right) = \gamma (s_b - d_b), \quad (11)$$

where s_b and d_b are the partial derivatives of the normalized growth and mortality functions, λ is a single eigenvalue of the system, and $|_*$ indicates evaluation at the steady state B^* . The system is stable if $\lambda < 0$ and unstable if $\lambda > 0$. As λ moves upwards toward 0, the system approaches a saddle-node bifurcation (Guckenheimer and Holmes 1983; Mangel 2006b), a critical transition associated with the sudden appearance of a stable and unstable fixed point, changing the dynamics rapidly (Kuznetsov 1998).

The linearization of Eq. 10 reveals two additional parameters, s_b and d_b , which are the partial derivatives of the normalized functions $s(b)$ and $d(b)$, respectively. Partial derivatives of normalized functions are equivalent to the *elasticities* of the unnormalized functions (Gross and Feudel 2006; Yeakel et al. 2011), which we show below. In general, elasticities provide a measure of the percent change of a function (e.g., consider the arbitrary function $F(X)$) relative to the percent change in its argument (X), where

$$\begin{aligned} \text{Elasticity}\{F(X)\} &= \frac{X}{F(X)} \frac{\partial F(X)}{\partial X} \\ &= \lim_{Y \rightarrow X} \frac{F(Y) - F(X)}{Y - X} \frac{X}{F(X)} \\ &= \lim_{Y \rightarrow X} \frac{1 - \frac{F(Y)}{F(X)}}{1 - \frac{Y}{X}} \approx \frac{\% \Delta F(X)}{\% \Delta X}. \end{aligned} \quad (12)$$

Elasticities can thus be thought of as dynamic measures that describe how a function responds to a perturbation and are commonly used in metabolic control theory (Fell 1992), economics (Sydsaeter and Hammond 1995), and life history theory (Horvitz et al. 1997). The elasticity of $F(X)$ with respect to its steady-state X^* is alternatively written as the logarithmic derivative of the function with respect to X^* (Yeakel et al. 2011) and is equivalent to the partial derivative of the normalized function $f(x)$,

$$f_x = \frac{X^*}{F^*} \left. \frac{\partial F}{\partial X} \right|_* = \left. \frac{\partial \log F}{\partial \log X} \right|_* = \left. \frac{\partial f}{\partial x} \right|_*. \quad (13)$$

Elasticities offer a number of advantages that are particularly useful for generalized modeling. First, an elasticity of a power-law function of the form $F(X) = aX^p$ is equal to p . This can be shown by normalizing $F(X)$ to the equilibrium X^* and taking the derivative at the steady state to obtain

$$f_x = \left. \frac{\partial f}{\partial x} \right|_* = \left. \frac{\partial}{\partial x} \frac{aX^p}{aX^{*p}} \right|_* = \left. \frac{\partial}{\partial x} x^p \right|_* = p.$$

For instance, if the function $D(B) = zB$ and z is constant, then the elasticity is equal to unity; if the function is quadratic, the elasticity is equal to 2; for constant functions, the elasticity is equal to 0 (Gross and Feudel 2006). For more complex functions, the value of the elasticity may change with the value of the steady state (see below). Furthermore, the elasticities of functions governing the time-evolution of an animal population are the representative of the environmental conditions present during measurement. Thus, elasticities are not defined with respect to unmeasurable biological conditions that serve to bound traditional

functional relationships, such as half-maximum values or growth rates at saturation (Fell and Sauro 1985; Fell 1992).

Relating functional elasticities to the degree of compensation

The degree of compensation in the Shepherd function (Eq. 4) is controlled by the parameter n : if $n < 1$ the function is Ricker-like, if $n > 1$ the function is Cushing-like, and if $n = 1$ it is equivalent to the B-H function (Shepherd 1982). In a generalized modeling framework, the degree of compensation is related directly to the functional elasticity. Given that B^* is large enough to experience density-dependent effects, if the elasticity of growth $s_b < 0$ the population grows according to a Ricker-like function, if $s_b > 0$ the population grows according to a Cushing-like function, and if $s_b \rightarrow 0$ the population grows according to the B-H function. Thus, n and s_b are closely related, which can be shown by mapping the Shepherd function (Eq. 4) to the generalized model (Eq. 10), where

$$s(b) = \frac{S(B)}{S(B^*)} = \frac{\alpha B}{1 + \beta B^{1/n}} \cdot \frac{1 + \beta B^{*1/n}}{\alpha B^*} \\ = \frac{1 + \beta B^{*1/n}}{1 + \beta B^{*1/n} b^{1/n}} b.$$

The elasticity of growth is thus

$$s_b = \frac{\partial s(b)}{\partial b} = 1 - \frac{\beta B^{*1/n}}{n(1 + \beta B^{*1/n})}. \quad (14)$$

Equation 14 shows that the elasticity of growth depends on both the steady state biomass and the degree of compensation, enabling direct comparisons between Ricker-like, Cushing-like, and B-H functions and their corresponding elasticities. For example, as B^* increases, if $n > 1$ (Cushing), then $s_b > 0$; if $n < 1$ (Ricker), then $s_b < 0$; if $n = 1$ (B-H), $s_b \rightarrow 0$ (Fig. 1a, b). (This is more readily apparent if the quantity $(1/\beta B^{*1/n})(1/\beta B^{*1/n})^{-1}$ is factored into the rightmost term of Eq. 14.) Because the value of the elasticity holds for any function $S(B)$, this generalization is not isolated to the Shepherd equation, but extends to any function with degrees of compensation that can be categorized as “Ricker-like,” “Cushing-like,” or “BH-like.” Thus, when density-dependent effects are present, if the value of the elasticity s_b can be determined, a general functional family can be assigned to the observed recruitment dynamics. This is a key relationship, because assignment of the functional family does not depend on the specific architecture of a given function.

If we assume that recruitment follows a Shepherd function, the degree of compensation can be determined directly from

$$s_b = \frac{\gamma + \alpha(n-1)}{\alpha n}, \quad \text{or alternatively, } n = \frac{\gamma - \alpha}{\alpha(s_b - 1)}, \quad (15)$$

where as before, γ is the biomass turnover rate, and α is the recruitment rate at low biomass. From this relationship, we see that if $s_b < 1$, γ is constrained to vary between 0 and α if n is to remain positive. Because γ is the biomass loss rate, it is evident that values greater than α (the maximum growth rate independent of density dependent effects) imply extinction of the population.

The relationship between the elasticity of growth and the degree of compensation suggests that the Cushing SRR and Ricker SRR are qualitatively different than the B-H SRR. The reasoning for this is straightforward: the elasticity of growth is a continuous variable, and recruitment following the B-H function is defined by the elasticity $s_b = 1$, whereas Cushing-like and Ricker-like functions have elasticities that span a range of values. Mathematically, the elasticities of the Ricker- and Cushing-like functional families can be represented by non-overlapping intervals (Ricker: $s_b \in [-\infty, 0)$; Cushing: $s_b \in (0, \infty]$). If we assume that observations of functional elasticities are normally distributed with a mean value of \bar{s}_b , and variability proportional to the difference between the mean and the boundary between Ricker, B-H, and Cushing SRRs ($s_b = 0$), using Eq. 14 to define \bar{s}_b , we obtain an equation for the frequency distribution of observed elasticities as a function of the steady state biomass

$$\delta_{B^*}(s_b) = \frac{1}{\sqrt{2\pi}} \frac{\exp\left(-\frac{(\beta B^{*1/n}(n(s_b-1)+1)+n(s_b-1))^2}{2(\beta B^{*1/n}(n-1)+n)^2}\right)}{\left[\frac{n}{\beta B^{*1/n}} + n\right]^{-1} - 1}. \quad (16)$$

If the steady state biomass is small, the distributions for the elasticities of Ricker, B-H, and Cushing SRRs ($n < 1$, $n = 1$, $n > 1$, respectively) are all centered at unity; as the steady state biomass increases, the distributions become centered at elasticities less than zero, equal to zero, and greater than zero, for Ricker, B-H, and Cushing SRRs, respectively. In the case of the B-H SRR, we observe that the distribution becomes centered at $s_b = 0$, while its standard deviation becomes infinitesimally small as B^* increases, such that in the limiting case of $B^* \rightarrow \infty$, $\delta_{B^*}(s_b)$ is a Dirac delta function (Dirac 1958). Thus, as the steady state increases, the probability of correctly measuring the elasticity goes to zero, emphasizing the observation that the B-H SRR is qualitatively different than the Ricker or Cushing

SRRs, and represents a boundary separating larger families of functional forms.

The discrimination of different governing functional forms (or families of functional forms) from observational data typically requires measures of statistical best fit using multiple years of stock-recruitment data (Munch et al. 2005). Because these data are often highly variable and complicated by changes in birth and death rates over long timespans, distinguishing between functional forms can be problematic. Because the elasticities of alternative functional families have non-overlapping ranges at intermediate to high levels of spawning stock biomass, they may be useful for determining the effects of density dependence on recruitment (Fig. 1). Moreover, because the sign of the elasticity can differentiate between competing functional families, the determination of functional family from the elasticity of growth may be relatively error-tolerant.

Measuring elasticities from time-series

We have shown that the degree of compensation can be calculated if the elasticity of growth is known. There exists a large body of literature in metabolic control theory for measuring elasticities in experimental settings (Fell 1992). However, these tools are not always appropriate for obtaining measurements from animal populations in the wild. We now show that the elasticity of growth can be measured from relatively small perturbations in fish biomass, and we provide a basic example using simulated data.

To begin, we consider single-species dynamics, where $dX/dt = F(X)$. We define deviation from the steady state, such that the population size at time t is some distance away from the equilibrium X^* as $\xi(t) = X(t) - X^*$. Then to first order $d\xi(t)/dt \approx F'(X^*)\xi$. $F'(X^*)$ is also the single eigenvalue of the system, λ_f , and we use the subscript f to distinguish the eigenvalue in this example from the eigenvalue λ defined for the production model. Integrating $d\xi(t)/dt$, we find that $\xi(t) = \xi_0 e^{\lambda_f t}$ where ξ_0 is the initial deviation and $X(t) = X^* + \xi_0 e^{\lambda_f t}$. Thus, the eigenvalue of a single-species system is equivalent to the rate of relaxation to the steady state of the population trajectory after a small perturbation if $\lambda_f < 0$.

Our generalized analysis of Eq. 5 shows that $\lambda = \gamma(s_b - d_b)$. For now, we will assume that λ can be measured. To determine which of the three functional families depicted in Fig. 1a drive recruitment dynamics, we must determine the elasticity of growth, where $s_b = \lambda/\gamma + d_b$. If mortality is assumed to be governed by a linear function, such that $d_b = 1$, then the criteria are simply defined by comparing the magnitude of the relaxation rate, λ , to the timescale of the system, γ (Table 1). If we assume that the steady state is stable ($\lambda < 0$), recruitment is driven by a Ricker-like function if $\lambda < -\gamma$, recruitment is driven by the B-H function if

$\lambda = -\gamma$, and recruitment is driven by a Cushing-like function if $\lambda > -\gamma$ (Fig. 1a). Because we do not presume to know the exact architecture of the stock-recruitment function, these relationships are predictive of general families of models. If we assume that growth is governed by the Shepherd function, the general relationship between the degree of compensation and the relaxation rate (cf. Eq. 15) is

$$n = \gamma \frac{\gamma - \alpha}{\alpha(\lambda + \gamma d_b - \gamma)} \tag{17}$$

which can be simplified further assuming that mortality is governed by a linear function, to give

$$n = \gamma \frac{\gamma - \alpha}{\alpha\lambda} \tag{18}$$

As the system approaches the saddle-node bifurcation at $\lambda = 0$, small errors in λ are likely to generate large errors in the degree of compensation (Eq. 18, Fig. 2), such that Ricker-like SRRs should result in measurements that

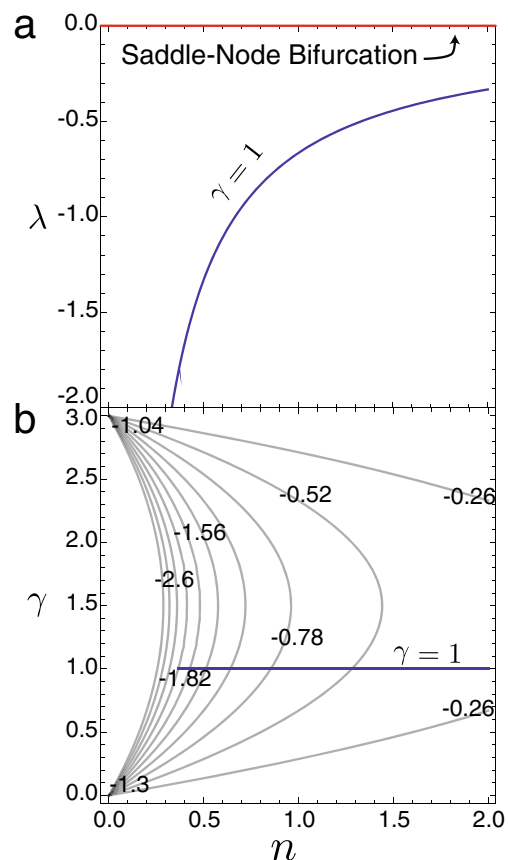


Fig. 2 **a** The rate of relaxation to the steady state λ versus the degree of compensation n for a biomass turnover rate $\gamma = 1$. The red line at $\lambda = 0$ denotes a saddle-node bifurcation below which the system is stable and above which the system is unstable. **b** The biomass turnover rate γ as a function of the degree of compensation n and the rate of relaxation λ (contour lines). The trajectory shown in **a** is denoted by the blue line. Values of $0 < \gamma < (\alpha = 3)$ result in stable dynamics, and only Cushing-like functions, where $n > 1$ can result in values of λ close to the saddle-node bifurcation

are more error-tolerant than Cushing-like SRRs. Moreover, because an elasticity of growth $s_b < 1$ produces dynamics with a single non-trivial stable steady state (assuming the elasticity of mortality $d_b = 1$), only Cushing-like SRRs can come close to the saddle-node bifurcation at $\lambda = 0$. The rate at which the saddle-node bifurcation is reached as n increases is contingent on the biomass turnover rate γ , where turnover rates intermediate to 0 and α approach the bifurcation more slowly. If the turnover rate is greater than α , $\lambda > 0$ and the system is unstable.

Estimating the degree of compensation from fluctuations in fish biomass

We have derived a relationship between the degree of compensation n and the elasticity of growth s_b , and have shown how—in principle—elasticities could be measured from short-term fluctuations in time-series data. To elaborate this idea, we constructed a stochastic model with growth following the Shepherd function and mortality due to both natural causes M and fishing F , coupled with observation error. We perturbed the system at time $t = t_i$ by eliminating the fishing mortality term (the end of a fishing period) until a steady state was reached at the terminal time $t = T$. We included normally distributed observation error \tilde{P} with mean zero and standard deviation σ . Accordingly, observations of fish biomass $B_{\text{obs}}(t)$ are then

$$\frac{d}{dt}B = \frac{\alpha B}{1 + \beta B^{1/n}} - (M + \delta_f F)B,$$

$$B_{\text{obs}}(t) = B(t) + \sigma \tilde{P},$$

where δ_f controls fishing mortality. During the fishing time interval $t_0 \leq t < t_i$, $\delta_f = 1$; during the non-fishing time interval $t_i \leq t < T$, $\delta_f = 0$ (Fig. 3).

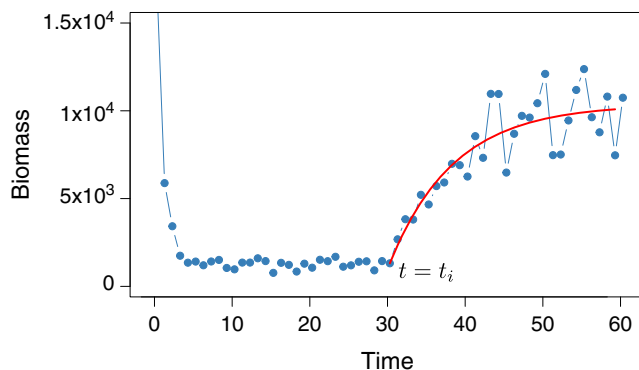


Fig. 3 An example of the transition from a fishing to a non-fishing interval used to measure the rate of relaxation λ from time-series data. The non-fishing interval is initiated at $t = t_i$, and biomass values immediately after t_i can be used to find the maximum likelihood estimate for λ . The best-fit trajectory using the likelihood technique is shown in red

Given the Gaussian assumption about the observation error, we assume that the system trajectory behaves as $B_{\text{obs}}(t) \sim N\{c(1 - e^{-\lambda t}), \sigma\}$ close to the steady state. The stochastic trajectory thus depends on the unknown variables c , λ , and σ , which we determine using a likelihood approach where k is the number of observations from the end of the fishing period until the trajectory reaches its steady state in the absence of fishing at $t = T$. This problem can be simplified, as the variables c and σ can be written in terms of λ to obtain the log-likelihood (Hilborn and Mangel 1997)

$$\log \mathcal{L}(\lambda) = -\frac{k}{2} \log(2\pi) - \frac{k}{2} \log \left\{ \frac{1}{k} \left(\sum_{t=t_i}^T B(t) - c(1 - e^{-\lambda t}) \right)^2 \right\} - \frac{k}{2}, \tag{19}$$

where $c = \sum_{t=t_i}^T B(t)(1 - e^{-\lambda t}) / \sum_{t=t_i}^T (1 - e^{-\lambda t})^2$. This relationship is then used to find the maximum likelihood estimate for the eigenvalue λ_{MLE} .

We aim to discriminate between different families of functional forms using the maximum likelihood estimate for the rate at which a population trajectory returns to its steady state after a perturbation. When the rate of relaxation is known, the degree of compensation can be calculated from Eq. 18. To determine the accuracy of our model estimates across different degrees of observation noise, we calculated λ_{MLE} as a function of the coefficient of variation ($\text{CV} = \sigma/B^*$) for three compensation scenarios: Ricker ($n = 0.5$), Cushing ($n = 1.5$), and B-H ($n = 1$). After estimating λ_{MLE} , we calculated the degree of compensation, n_{MLE} from Eq. 18, and determined the probability that the correct value of n was estimated with an accuracy of ± 0.2 (Fig. 4a,b), as well as the probability that the functional family was correctly identified (Fig. 4a,c).

Results

Sensitivity to observation error

The analytical relationship between the degree of compensation n and the elasticity of growth s_b (Eq. 18) suggests that populations growing in accordance to Ricker-like functions should be less difficult to measure accurately than those growing in accordance to Cushing-like functions (Fig. 2a). Our simulation experiment showed that the rate of relaxation can be estimated from moderately noisy data and that there were large differences in the measurement accuracy for different functional families. As predicted, the estimated rate of relaxation λ_{MLE} , and by transformation n_{MLE} , is estimated more accurately for Ricker-like and B-H functions than for Cushing-like functions (Fig. 4a). We note that the

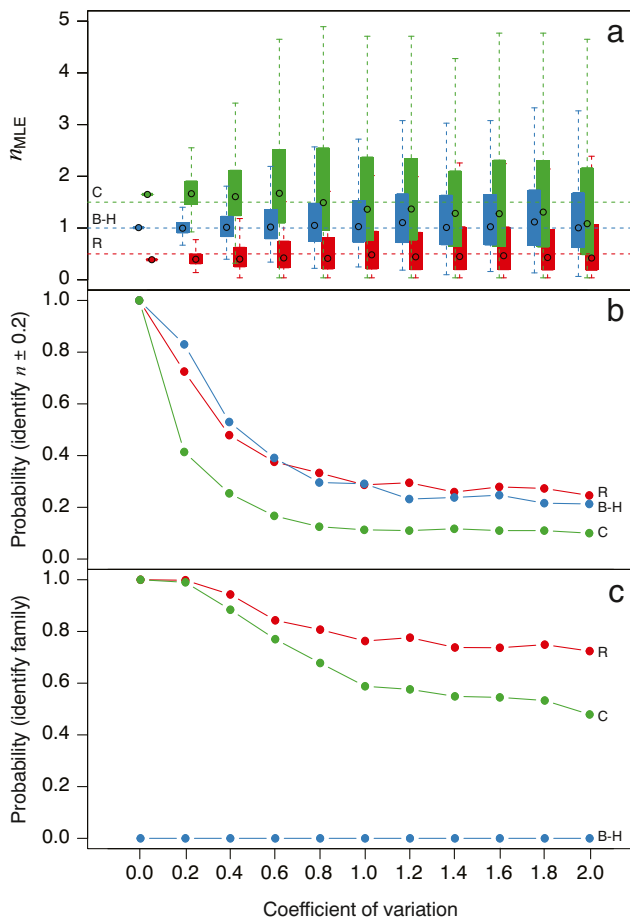


Fig. 4 **a** Estimation of the degree of compensation as a function of the coefficient of variation for simulated population trajectories (1,000 replicates); Ricker (R), red; Beverton-Holt (B-H), blue; Cushing (C), green; circles denote medians. **b** The probability of correctly estimating the degree of compensation within a certain amount of error (Ricker: $n = 0.5 \pm 0.2$; B-H: $n = 1 \pm 0.2$), and Cushing: $n = 1.5 \pm 0.2$. **c** The probability of correctly estimating the correct SRR family (Ricker: $n < 1$; B-H: $n = 1$; Cushing: $n > 1$)

mean value of our estimates always diverged from the set value of n because the rate of return equation is only accurate at values very close to B^* and is therefore a necessarily crude estimate of the solution to $B_{\text{obs}}(t)$.

The probability that the degree of compensation was estimated to within ± 0.2 of the set value declined nonlinearly for all SRRs, asymptoting at a probability of ≈ 0.2 for Ricker and B-H, and ≈ 0.1 for Cushing at $CV = 2$, the latter result due primarily to the greater range of n defining the Cushing functional form (Fig. 4b). Perhaps the more important issue relates to the probability that the functional family can be correctly determined with respect to other functional families. Our results showed that the probably of correctly determining the functional family from λ_{MLE} remained relatively high as the CV increased (Fig. 4c) for both Ricker-like and Cushing-like functions. The probability that Ricker-like

functions were correctly distinguished was generally greater than 0.8 for $CV \leq 2$, while the probability that Cushing-like functions were correctly distinguished was greater than 0.5 for $CV \leq 2$. Because the B-H function is a boundary between functional families (see Methods), the probability that it was correctly distinguished was always 0.

Sensitivity to time-series length and process stochasticity

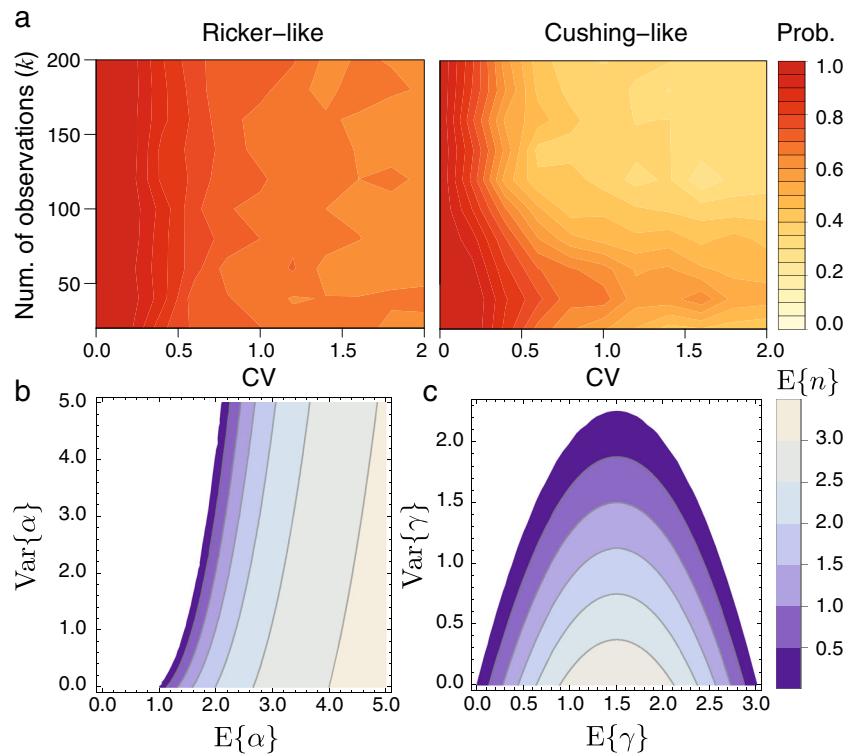
The accuracy of measurements for the elasticity of growth in the field will depend on the additional sources of bias and variability other than observation error. In particular, we briefly examine two important sources of variability that may impact estimation accuracy (1) the number of observations in a time-series and (2) variability of the intrinsic growth rate α (process noise) and the biomass turnover rate γ .

The number of observations in a time-series k is used in Eq. 19 to calculate the maximum likelihood estimate for λ ; changes in k will thus affect estimates of λ . To test this, we performed a simulation experiment, where we calculated the probability of correctly identifying Ricker-like versus Cushing-like SRRs as a function of both CV and the number of observations. We found that, as long as the population reproduces quickly enough to attain its post-perturbation equilibrium within the time-frame in question (this is a fundamental feature of our approach), the number of observations does not adversely affect the use of elasticities to estimate the nature of compensation (Fig. 5a).

Variability in the intrinsic growth rate of a population is a common source of uncertainty, particularly for populations spanning multiple spawning grounds or where primary productivity is prone to seasonal or annual fluctuations (Mangel 2006a; Dorner et al. 2008). In contrast to variability in the number of observations, we can derive an analytical approximation for the effect that process noise and timescale variability have on estimating the degree of compensation. To determine how variability in α and γ influences our estimation of the degree of compensation, we first establish α and γ as random variables and solve for the expectation of the degree of compensation, $E\{n\}$, as a function of the expectation and variance of α ($E\{\alpha\}$ and $\text{Var}\{\alpha\}$, respectively), the biomass turnover rate γ ($E\{\gamma\}$ and $\text{Var}\{\gamma\}$, respectively), and the covariance between α and γ ($\text{Cov}\{\alpha, \gamma\}$). The expectation can be approximated by implementing the Delta Method (Hilborn and Mangel 1997), so that to second order

$$E\{n\} \approx \frac{1}{\lambda E\{\alpha\}^3} \left(E\{\gamma\} \left[E\{\alpha\}^3 + 2E\{\alpha\}\text{Cov}\{\alpha, \gamma\} - E\{\gamma\} \left(E\{\alpha\}^2 + \text{Var}\{\alpha\} \right) \right] - E\{\alpha\}^2 \text{Var}\{\gamma\} \right). \tag{20}$$

Fig. 5 **a** The probability of correctly identifying Cushing-like and Ricker-like functional families as a function of observation error CV = 0 to 2 and the number of observations $k = 20$ to 200. **b** $E\{n\}$ as a function of $E\{\alpha\}$ versus $\text{Var}\{\alpha\}$. **c** $E\{n\}$ as a function of $E\{\gamma\}$ versus $\text{Var}\{\gamma\}$



If we assume that $\text{Cov}\{\alpha, \gamma\}$ is small, we observe that as $\text{Var}\{\alpha\}$ increases, the degree of compensation changes only slowly, which in turn is dampened as α becomes larger (Fig. 5b). Thus, we find that variability in the growth rate does not have a large influence on estimating the degree of compensation, except when the system is close to the saddle-node bifurcation at $\alpha = \gamma$.

As expected from the relationship defined between λ and γ (Table 1), we find that it is more important to constrain estimates of the characteristic timescale of the population dynamics (Fig. 5c) or in this case the biomass turnover rate. Obtaining accurate measurements of the characteristic timescale of population dynamics is essential for determining system behavior in many contexts (Auger and Poggiale 1996; Mchich et al. 2002) and is a strict requirement for

the utilization of the approach that we describe here. The biomass turnover rate for a population can be estimated in a variety of direct and indirect ways. For example, biomass turnover tends to vary predictably with species body mass (Calder 1996), and allometric scaling relationships may prove useful for determining an initial baseline for γ . Direct measurement of biomass turnover can be approached via tag-recovery or capture-recapture methods (Kleiber et al. 1987), and because the inverse of γ is the average life-expectancy of individuals within the population, could be estimated from sequential measures of body mass or length distributions. Although we do not treat this issue in detail here, combining these approaches within a Bayesian hierarchical model would permit the biomass turnover rate to be expressed as a distribution, thus related to the expectation for the degree of compensation as presented in Eq. 20.

Table 1 Criteria for determining the elasticity of growth s_b from the rate of return to the steady state after a perturbation, λ , for the production model

Model	Elasticity ($B^* \gg 0$)	Criterion
Ricker-like	$s_b < 0$ s.t. $\frac{\lambda}{\gamma} + d_b < 0$	$\lambda < -\gamma d_b$
Beverton-Holt	$s_b = 0$ s.t. $\frac{\lambda}{\gamma} + d_b = 0$	$\lambda = -\gamma d_b$
Cushing-like	$s_b > 0$ s.t. $\frac{\lambda}{\gamma} + d_b > 0$	$\lambda > -\gamma d_b$

The non-overlapping intervals for the elasticity of growth uniquely identify of Ricker-like, Beverton-Holt, and Cushing-like recruitment dynamics

An example with age structure

Production models effectively summarize the recruitment dynamics of fish populations and in some cases can provide robust measures of fisheries reference points (MacCall 2002; Mangel et al. 2010, 2013). However, the influence of age-related differences in growth and mortality can have large effects on the dynamics of fish populations (Mangel et al. 2006; Shelton and Mangel 2011). In this

section, we build upon our prior results and expand the generalized modeling schema to discrete time, age-structured models. The extension of generalized modeling to discrete time systems is useful in its own right, as it provides a method for the dynamical analysis of whole classes of discrete time models (*sensu* Gross and Feudel 2006). First, we briefly illustrate an extension of the generalized modeling approach to an age-structured discrete time system. Second, we show how the degree of compensation in an age-structured system is related to the elasticities of growth and finish by showing how measurements of elasticities in the age-structured model provide important insight into system stability.

We consider an age-structured model where the number of recruits $X(t + 1)$ is governed by spawning stock biomass, $B_s(t)$, depending on the degree of compensation n . The number of individuals in the mature age class Y is the sum of returning adults and incoming recruits, where adult mortality is given by M_y and recruit mortality is given by M_x . It follows that spawning stock biomass is calculated by the number of mature individuals times the average mass of individuals W_y . The age-structured model is thus

$$\begin{aligned} X(t + 1) &= F(B_s, t) &&= \frac{\alpha B_s(t)}{1 + \beta B_s(t)^{1/n}}, \\ Y(t + 1) &= G(X, t) + H(Y, t) &&= X(t)e^{-M_x} + Y(t)e^{-M_y}, \\ B_s(t + 1) &= K(Y, t) &&= Y(t)W_y. \end{aligned} \quad (21)$$

We can determine the steady state condition X^* (where $X(t + 1) = X(t)$) in terms of spawning stock biomass B_s^* because at the steady state $B_s^* = Y^*W_y$, such that

$$B_s^* = X^* \frac{e^{-M_x} W_y}{1 - e^{-M_y}} = X^* W_f^*. \quad (22)$$

The primary difference between the age-structured and production models is that mortality is not assumed to occur simultaneously with recruitment, and this yields dynamics that diverge strongly from those predicted by the production model. We note that this 3-dimensional model can be slightly modified and collapsed such that $B_s(t) = Y(t)W_y$, and this has a little effect on the qualitative dynamics.

The normalization of the age-structured system is analogous to the normalization of the production model (Eq. 7), however because the age-structured system is composed of difference rather than differential equations, the steady state condition requires that the scale parameters are defined differently than before. For example, $y(t + 1) = (G^*/Y^*)g(x, t) + (H^*/Y^*)h(y, t)$ is defined at the steady state $1 = G^*/Y^* + H^*/Y^*$, such that we define the ratio of incoming recruits to the abundance of the mature age-class $\gamma_y = G^*/Y^*$ and the ratio of returning adults to the abundance of the mature age-class $(1 - \gamma_y) = H^*/Y^*$. These coefficients are thus the proportional contributions of recruit

and mature age-classes to spawning stock biomass at the steady state. The generalized system is then

$$\begin{aligned} x(t + 1) &= \gamma_x f(b, t), \\ y(t + 1) &= \gamma_y g(x, t) + (1 - \gamma_y)h(y, t), \\ b(t + 1) &= \gamma_b k(y, t). \end{aligned} \quad (23)$$

We can immediately simplify the problem by observing that the scale parameters for recruits and biomass can be reduced to

$$\begin{aligned} \gamma_x &= \frac{F^*}{X^*} = \frac{\alpha W_f^*}{1 + \beta (W_f^* X^*)^{1/n}} = 1, \\ \gamma_b &= \frac{K^*}{B_s^*} = 1. \end{aligned} \quad (24)$$

For the production model, elasticities were defined with respect to the linearized system (Eq. 11). Because the age-structured system is multi-dimensional, the linearization is defined by the Jacobian matrix evaluated at the steady state $\mathbf{J}|_*$, where each element is defined by the partial derivative of each difference equation with respect to each variable. The elasticities of the generalized system can then be calculated, such that

$$\mathbf{J}|_* = \begin{pmatrix} \left. \frac{\partial F}{\partial X} \right|_* & \left. \frac{\partial F}{\partial Y} \right|_* & \left. \frac{\partial F}{\partial B_s} \right|_* \\ \left. \frac{\partial G+H}{\partial X} \right|_* & \left. \frac{\partial G+H}{\partial Y} \right|_* & \left. \frac{\partial G+H}{\partial B_s} \right|_* \\ \left. \frac{\partial K}{\partial X} \right|_* & \left. \frac{\partial K}{\partial Y} \right|_* & \left. \frac{\partial K}{\partial B_s} \right|_* \end{pmatrix} = \begin{pmatrix} 0 & 0 & f_b \\ \gamma_y & (1 - \gamma_y) & 0 \\ 0 & 1 & 0 \end{pmatrix}, \quad (25)$$

where for the specific age-structured model, $\gamma_y = 1 - e^{-M_y}$, and the elasticity of growth is

$$f_b = \left. \frac{\partial f(b)}{\partial b} \right|_* = \frac{\alpha W_f^* (n - 1) + 1}{\alpha W_f^* n}. \quad (26)$$

The Jacobian matrix determines the stability of the system; we solve for the eigenvalues that satisfy the characteristic equation $\text{Det}(\mathbf{J}|_* - \lambda \mathbf{I}) = 0$, where \mathbf{I} is the identity matrix. From Eq. 26, the characteristic equation is $f_b \gamma_y + \lambda^2 - \gamma_y \lambda^2 - \lambda^3 = 0$, which yields three distinct eigenvalues, and though the solutions for these eigenvalues are large and unwieldy, they can be easily derived with algebraic computing languages such as Maple or Mathematica. We have thus derived a generalization for the stability of the age-structured model with two measurable parameters: the proportional contribution of recruits to the adult age class γ_y and the elasticity of growth f_b . We note that, in theory, the elasticity of growth in the age-structured case can be estimated from time-series data as before, but where the rate of return after a perturbation is measured across two dimensions: the number of recruits versus the number of adults.

Simulation of the specific age-structured system (where $\alpha = 8$, $\beta = 1/80$, $M_x = 0.2$, $M_y = 0.7$, and $W_y = 2$) across a range of values for the degree of compensation

reveals a single steady state for $n > 0.376$. For $n < 0.376$, stable cycles emerge, which in turn give rise to five-period cycles for lower values of n (Fig. 6a,b). In discrete time systems, the emergence of cyclic conditions can result from crossing a Neimark–Sacker bifurcation (cf. Guill et al. 2011a, b), which occurs when a pair of complex conjugate eigenvalues cross the unit circle on the complex plane. If λ_1 and λ_2 are the complex conjugate eigenvalue pair, the test function for this condition is $\lambda_1\lambda_2 = 1$ (Kuznetsov 1998). Using solutions for λ_1 and λ_2 from the characteristic equation, we numerically determined that a supercritical Neimark–Sacker bifurcation is crossed at $n = 0.376$ (Fig. 6a,c). Supercritical Neimark–Sacker bifurcations yield stable closed invariant curves, such that local trajectories initiated interior and exterior to the cycle are attracted to the curve (Fig. 6b; Kuznetsov 1998). Predictions of population dynamics are thus possible, but only if the degree of compensation, in addition to the other parameters, is known. As with the specific production model, the specific age-structured model introduces strong assumptions regarding functional forms, and these assumptions may not hold (or be conducive to measurement) in many situations.

Because the degree of compensation is related directly to the elasticity of growth (Eq. 26), we can use the generalized age-structured system to gather direct insight

into the potential dynamics applicable to any class of models substituted into the general functions $F(B)$, $G(X)$, $H(Y)$, and $K(Y)$. Although the test function for the Neimark–Sacker bifurcation is not analytically tractable (even for the generalized system), we can numerically simulate the relationship between the elasticity of growth f_b , the proportion of maturing recruits to the mature age class γ_y (which has a value of 0.50 in the simulated age-structured model), and the test-function $\lambda_1\lambda_2$.

Our numerical results show that only Ricker-like SRRs can result in cyclic dynamics ($\lambda_1\lambda_2 \geq 1$; Fig. 6d). Moreover, we observe that cyclic dynamics can only emerge if $f_b \leq -1$ for any potential value of γ_y , and this result applies to all potential SRRs. Accordingly, as the ratio of maturing recruits declines (low γ_y ; realized as the mortality of the mature age-class M_y decreases), cyclic dynamics are less likely to occur unless the elasticity of growth is extremely low, which is biologically unreasonable. As the ratio of maturing recruits increases (higher mature age-class mortality), the opposite occurs, and cyclic dynamics are more likely for a broader range of Ricker-like SRRs. We have thus obtained a very powerful result: independent of the particular functions introduced into the general age-structured system, cyclic dynamics require (1) that spawning stock biomass includes a relatively large proportion of incoming recruits and 2) that compensatory

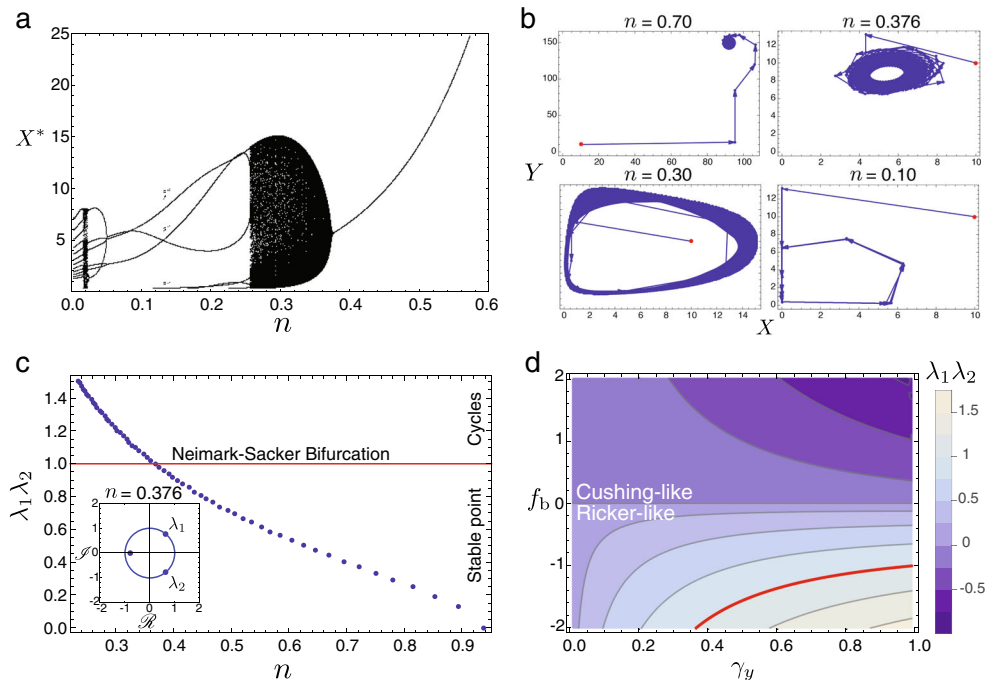


Fig. 6 **a** Bifurcation diagram showing the onset of cycles followed by multi-period oscillations for the age-structured model as the degree of compensation lowers beyond $n = 0.376$. **b** Examples of the corresponding dynamics where $n = 0.70, 0.376, 0.30,$ and 0.10 . **c** Values of the test-function $\lambda_1\lambda_2$ across different values of n for the specific model. A Neimark–Sacker bifurcation exists at $\lambda_1\lambda_2 = 1$, which is

crossed at $n = 0.376$. This condition exists when two complex conjugate eigenvalues cross the unit circle on the complex plane (inset). **d** Numerically estimated values for the test-function $\lambda_1\lambda_2$, given the elasticity of growth f_b and the ratio of incoming recruits to the mature age-class γ_y . The *red contour* denotes the Neimark–Sacker bifurcation condition; systems below this contour have cyclic dynamics

dynamics are driven by a Ricker-like function, where the elasticity of growth has a value ≤ -1 .

The relationship between recruitment, the elasticity of growth, and cyclic dynamics has predictive power, in particular because it is general without assumptions regarding the exact shapes of functional responses. For example, pink salmon (*Oncorhynchus gorbuscha*) are a widespread species with complex population dynamics (Radchenko et al. 2007). Depensatory dynamics are responsible for a large source of embryo mortality as spawning individuals compete for viable nests, such that Ricker-like models are generally predictive of stock recruitment relationships (May 1974; Myers et al. 1995). Moreover, pink salmon are semelparous, such that there is a little or no overlap in spawning stock biomass between generations. In our generalized modeling framework, this corresponds to an elasticity of growth $f_b < 0$, and complete turnover of the adult age-class, such that γ_y is close to unity. From Fig. 6d, we observe that cyclic dynamics are inevitable if $f_b < -1$ as $\gamma_y \rightarrow 1$. In nature, pink salmon populations are strongly cyclic, generally on the order of 2-year cycles, and this is thought to be caused by density-dependent mortality reinforced by external sources of stochasticity (Krkosek et al. 2011). Thus, we observe that by relating the elasticity of growth to stability regimes, knowledge of general aspects of population dynamics—without assuming specific functional relationships—can provide direct insights into the compensatory dynamics of age-structured populations.

Discussion

We have shown that the elasticity of growth in a generalized production model can be related directly to the degree of compensation parameter that determines Ricker-like, Cushing-like, or Beverton-Holt behaviors. The elasticity of growth is useful because it is defined with respect to the biological and environmental conditions present during measurement, and thus can be estimated from limited time-series data. Moreover, because large ranges of the elasticity of growth, and by extension the rate of relaxation, characterize families of functional forms, these measures are relatively error tolerant (Fig. 4c), particularly if the goal is to distinguish between SRRs with Ricker-like or Cushing-like recruitment dynamics.

The functional elasticities of both production and age-structured models can be used to determine directly the compensatory dynamics driving SRRs. This method may be of most use to recent fisheries, where long-term time-series data do not yet exist. Because we have employed elasticities in a generalized modeling framework, they are well-suited to inform knowledge of the general nature of compensation, and thus may be particularly useful for developing

priors for parameters in flexible SRRs, such as the degree of compensation in the Shepherd model.

Our exploration of elasticities operates under the expectation of shifting-equilibrium dynamics, thus assuming that there are strong regulatory mechanisms driving the reproductive dynamics of populations (Murdoch 1994). This assumption should have local validity over short timescales. Moreover, the approach does not assume a specific equilibrium (thus holding for all potential equilibria) such that it may be applicable to populations under constant perturbations, where the equilibrium is a moving target. Although estimating the rate of relaxation necessarily requires that the system has attained (or is approaching) a post-perturbation steady state, important information regarding the degree of compensation can be estimated even when the intrinsic variability approaches the same magnitude as the external perturbation (Fig. 4). This depends on some knowledge of what external forces—and the time-frame over which they operate—induce the perturbation, such that our example of using a moratorium on harvesting to estimate the rate of relaxation carries with it a certain practicality.

Elasticities describe the system in its current state. Accordingly, much can be learned about the nature of a population's compensatory dynamics if the elasticity of growth can be determined as the steady state shifts over time. We suggest that determining to what extent elasticities can be measured with respect to perturbations of different magnitudes and across different temporal spans may be of future research interest, as is investigating new and different ways to measure elasticities in wild populations.

Acknowledgements We thank S. Allesina, M.P. Beakes, D. Braun, T. Gross, C. Kuehn, T. Levi, A. MacCall, J.W. Moore, S. Munch, M. Novak, C.C. Phillis, and A.O. Shelton for many helpful discussions and comments. We also thank the Dynamics of Biological Networks Lab at the Max-Planck Institute for the Physics of Complex Systems and the University of Bristol for sharing the ideas and knowledge that inspired this work. This project was partially funded by the Center for Stock Assessment and Research, a partnership between the Fisheries Ecology Division, NOAA Fisheries, Santa Cruz, CA and the University of California, Santa Cruz and by NSF grant EF-0924195 to M.M.

References

- Auger P, Poggiale JC (1996) Emergence of population growth models: Fast migration and slow growth. *J Theor Biol* 182(2):99–108
- Beverton RJH, Holt SJ (1957) On the dynamics of exploited fish populations. Springer, New York
- Brooks EN, Powers JE (2007) Generalized compensation in stock-recruit functions: Properties and implications for management. *ICES J Mar Sci* 64(3):413–424
- Calder IIIWA (1996) Size, function, and life history. Courier Dover Publications, Cambridge
- Cushing DH (1973) The dependence of recruitment on parent stock. *J Fish Res Bd Can* 30:1965–1976

- Cushing DH (1988) The problems of stock and recruitment. In: Fish population dynamics: the implications for management. Wiley, New York
- Dirac PAM (1958) The principles of quantum mechanics. Clarendon Press, Oxford
- Dorner B, Peterman RM, Haeseker SL (2008) Historical trends in productivity of 120 Pacific pink, chum, and sockeye salmon stocks reconstructed by using a Kalman filter. *Can J Fish Aquat Sci* 65(9):1842–1866
- Fell DA (1992) Metabolic control analysis: a survey of its theoretical and experimental development. *Biochem J* 286(Pt 2):313–330
- Fell DA, Sauro HM (1985) Metabolic control and its analysis. *Eur J Biochem* 148(3):555–561
- Feynman R (1948) Space-time approach to non-relativistic quantum mechanics. *Rev Mod Phys* 20(2):367–387
- Gross T, Feudel U (2006) Generalized models as a universal approach to the analysis of nonlinear dynamical systems. *Phys Rev E* 73(1 Pt 2) 016:205
- Gross T, Rudolf L, Levin SA, Dieckmann U (2009) Generalized models reveal stabilizing factors in food webs. *Science* 325(5941):747–750
- Guckenheimer J, Holmes P (1983) Nonlinear oscillations, dynamical systems and bifurcations of vector fields. Springer, New York
- Guill C, Drossel B, Just W, Carmack E (2011a) A three-species model explaining cyclic dominance of Pacific salmon. *J Theor Biol* 276(1):16–21
- Guill C, Reichardt B, Drossel B, Just W (2011b) Coexisting patterns of population oscillations: the degenerate Neimark-Sacker bifurcation as a generic mechanism. *Phys Rev E* 83(2):021,910
- Gulland JA (1988) The analysis of data and development of models. In: Fish population dynamics: the implications for management. Wiley, New York
- Hilborn R, Mangel M (1997) The ecological detective: confronting models with data. Princeton University Press, Princeton
- Horvitz C, Schemske DW, Caswell H (1997) The relative “importance” of life-history stages to population growth: prospective and retrospective analyses. In: Structured-population models in marine, terrestrial, and freshwater systems. Chapman and Hall, New York, pp 247–271
- Johnson DW, Grorud-Colvert K, Sponaugle S, Semmens BX (2014) Phenotypic variation and selective mortality as major drivers of recruitment variability in fishes. *Ecol Lett* Early edition
- Kleiber P, Argue AW, Kearney RE (1987) Assessment of Pacific Skipjack Tuna (*Katsuwonus pelamis*) resources by estimating standing stock and components of population turnover from tagging data. *Can J Fish Aquat Sci* 44(6):1122–1134
- Krkosek M, Hilborn R, Peterman RM, Quinn TP (2011) Cycles, stochasticity and density dependence in pink salmon population dynamics. *Proc Roy Soc B* 278(1714):2060–2068
- Kuehn C, Siegmund S, Gross T (2013) Dynamical analysis of evolution equations in generalized models. *IMA J Appl Math* 78(5):1051–1077
- Kuznetsov Y (1998) Elements of applied bifurcation theory. Springer, New York
- MacCall AD (2002) Use of known-biomass production models to determine productivity of west coast groundfish stocks. *N Am J Fish Manage* 22(1):272–279
- Mangel M (2006a) An introduction to some of the problems of sustainable fisheries. In: The theoretical biologist’s toolbox: Quantitative methods for ecology and evolutionary biology. Cambridge University Press, Cambridge, pp 1–38
- Mangel M (2006b) The theoretical biologist’s toolbox: Quantitative methods for ecology and evolutionary biology. Cambridge University Press, Cambridge
- Mangel M, Marinovic B, Pomeroy C, Croll D (2002) Requiem for Ricker: Unpacking MSY. *B Mar Sci* 70(2):763–781
- Mangel M, Levin P, Patil A (2006) Using life history and persistence criteria to prioritize habitats for management and conservation. *Ecol Appl* 16(2):797–806
- Mangel M, Brodziak J, DiNardo G (2010) Reproductive ecology and scientific inference of steepness: a fundamental metric of population dynamics and strategic fisheries management. *Fish Fish* 11(1):89–104
- Mangel M, MacCall AD, Brodziak J, Dick EJ, Forrest RE, Pourzand R, Ralston S (2013) A perspective on steepness, reference points, and stock assessment. *Can J Fish Aquat Sci* 70(6):930–940
- Marshall CT (2009) Fish reproductive biology: implications for assessment and management. In: Jakobsen T, Fogarty MJ, Megrey BA, Moksness E (eds) Fish reproductive biology: Implications for assessment and management. Wiley-Blackwell, West Sussex, pp 395–420
- May RM (1974) Biological populations with nonoverlapping generations: Stable points, stable cycles, and chaos. *Science* 186(4164):645–647
- Mchich R, Auger PM, Bravo de la Parra R, Raissi N (2002) Dynamics of a fishery on two fishing zones with fish stock dependent migrations: Aggregation and control. *Ecol Model* 158(1–2):51–62
- Moore JW, Yeakel JD, Peard D, Lough J, Beere M (2014) Life-history diversity and its importance to population stability and persistence of a migratory fish: Steelhead in two large North American watersheds. *J Anim Ecol*
- Morgan MJ, Perez-Rodriguez A, Saborido-Rey F, Marshall CT (2011) Does increased information about reproductive potential result in better prediction of recruitment? *Can J Fish Aquat Sci* 68(8):1361–1368
- Munch SB, Kottas A, Mangel M (2005) Bayesian nonparametric analysis of stock-recruitment relationships. *Can J Fish Aquat Sci* 62(8):1808–1821
- Murdoch WW (1994) Population regulation in theory and practice. *Ecology* 75(2):271–287
- Myers RA, Barrowman NJ, Hutchings JA, Rosenberg AA (1995) Population dynamics of exploited fish stocks at low population levels. *Science* 269(5227):1106–1108
- Perretti CT, Munch SB, Sugihara G (2013a) Model-free forecasting outperforms the correct mechanistic model for simulated and experimental data. *Proc Natl Acad Sci USA* 110(13):5253–5257
- Perretti CT, Sugihara G, Munch SB (2013b) Nonparametric forecasting outperforms parametric methods for a simulated multispecies system. *Ecology* 94(4):794–800
- Radchenko VI, Temnykh OS, Lapko VV (2007) Trends in abundance and biological characteristics of pink salmon (*Oncorhynchus gorbuscha*) in the North Pacific Ocean. *North Pac Anadromous Fish Comm Bull* 4:7–21
- Ricker H (1954) Stock and recruitment. *Can J Fish Aquat Sci* 11(5):559–623
- Shelton AO, Mangel M (2011) Fluctuations of fish populations and the magnifying effects of fishing. *Proc Natl Acad Sci USA* 108(17):7075–7080
- Shepherd J (1982) A versatile new stock-recruitment relationship for fisheries, and the construction of sustainable yield curves. *J Conseil* 40(1):67
- Sissenwine MP, Shepherd JG (1987) An alternative perspective on recruitment overfishing and biological reference points. *Can J Fish Aquat Sci* 44(4):913–918
- Stiefs D, van Voorn GAK, Kooi BW, Feudel U, Gross T (2010) Food quality in producer-grazer models: a generalized analysis. *Am Nat* 176(3):367–380
- Sydsaeter K, Hammond PJ (1995) Essential mathematics for economic analysis. Prentice-Hall Inc., New Jersey
- Yeakel JD, Stiefs D, Novak M, Gross T (2011) Generalized modeling of ecological population dynamics. *Theor Ecol* 4(2):179–194